Supporting Information

Enhanced electrochemical catalysis and sensing applications: fabrication process optimization and electrocatalytic characterization of polymeric matrix composite for one-step synthesis of Pd nanoparticle-decorated laser-induced graphene electrodes

Asamee Soleh[a,b,c,d,e], *Kasrin Saisahas*[d,e], *Kiattisak Promsuwan*[a,d,e], *Jenjira Saichanapan*[d,e], *Panote Thavarungkul*[a,b,c], *Proespichaya Kanatharana*[a,b,c], *Lingyin Meng*[f], *Wing Cheung Mak*[f,g**], *Warakorn Limbut*[a,b,d,e*]

[a] Center of Excellence for Trace Analysis and Biosensor, Prince of Songkla University, Hat Yai, Songkhla, 90110, Thailand

[b] Center of Excellence for Innovation in Chemistry, Faculty of Science, Prince of Songkla University, HatYai, Songkhla, 90110, Thailand

[c] Division of Physical Science, Faculty of Science, Prince of Songkla University, Hat Yai, Songkhla, 90110, Thailand

[d] Division of Health and Applied Sciences, Faculty of Science, Prince of Songkla University, Hat Yai, Songkhla, 90110, Thailand

[e] Forensic Science Innovation and Service Center, Prince of Songkla University, Hat Yai, Songkhla, 90110, Thailand

[f] Division of Sensor and Actuator Systems, Department of Physics, Chemistry and Biology, Linköping University, Linköping, SE-581 83, Sweden

[g] Department of Biomedical Engineering, the Chinese University of Hong Kong, Hong Kong SAR, China

*Corresponding author at: Division of Health and Applied Sciences, Faculty of Science, Prince of Songkla University, Hat Yai, Songkhla 90110, Thailand.

E-mail addresses: warakorn.l@psu.ac.th (W. Limbut)

**Corresponding author at: Department of Biomedical Engineering, the Chinese University of Hong Kong, Hong Kong SAR, China

E-mail addresses: wing.cheung.mak@cuhk.edu.hk (W.C. Mak)

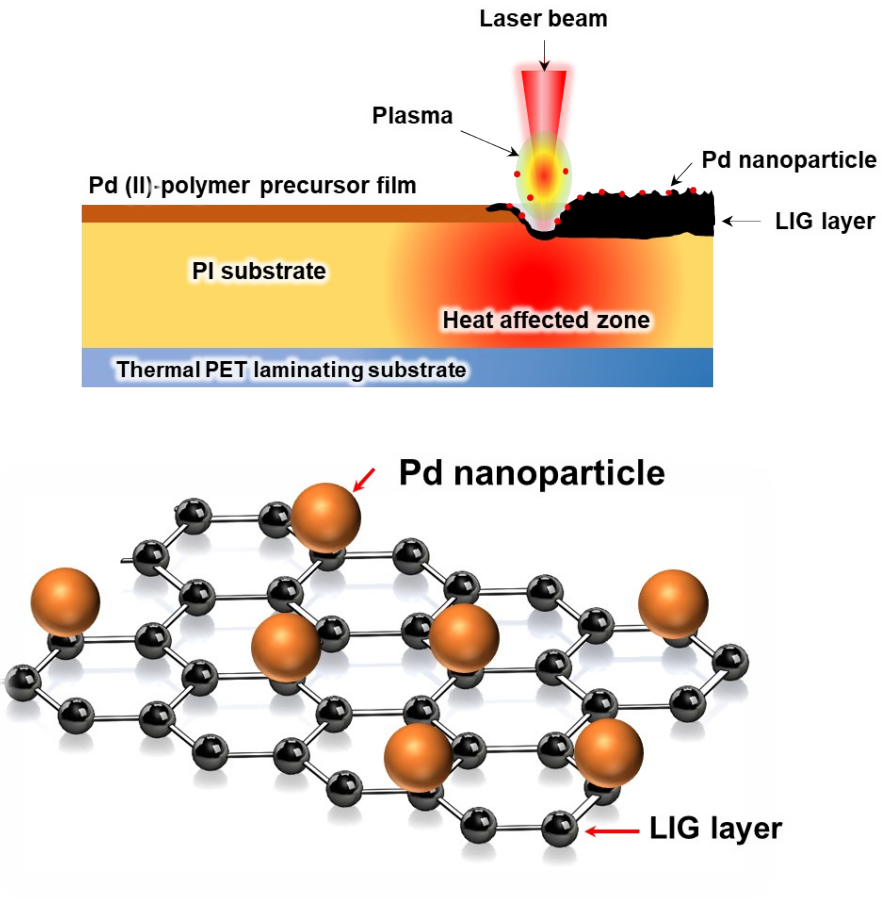

Schematic S1. Illustration of the laser induction process of Pd nanoparticles on the laser-induced graphene composite.

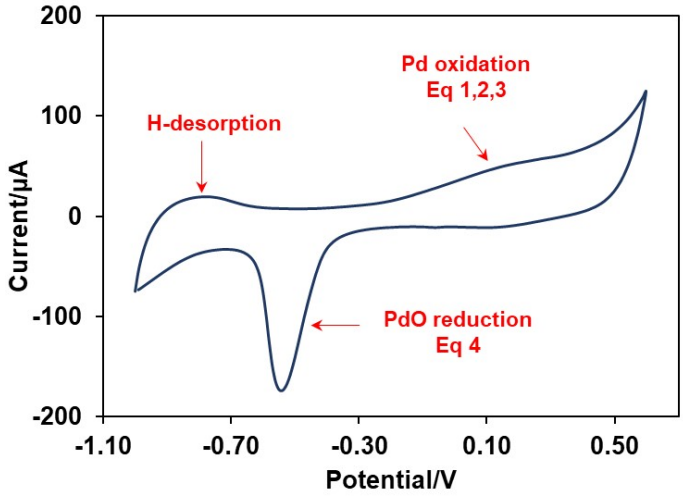

$$Pd + OH^- \longrightarrow Pd - OH_{ads} + H_2O + e^- \quad (1)$$

$$Pd - OH_{ads} + OH^- \longrightarrow Pd - O\ (Pd\ oxide) + H_2O + e^- \quad (2)$$

$$Pd - OH_{ads} + Pd - OH_{ads} \longrightarrow Pd - O\ (Pd\ oxide) + H_2O \quad (3)$$

$$Pd - O\ (Pd\ oxide) + H_2O + 2e^- \longrightarrow Pd + 2OH^- \quad (4)$$

Fig. S1. CV response of nanoPd@LIG at scan rate of 0.05 V s^{-1} in 0.1 mol L^{-1} KOH; and the reaction mechanism of nanoPd@LIG.

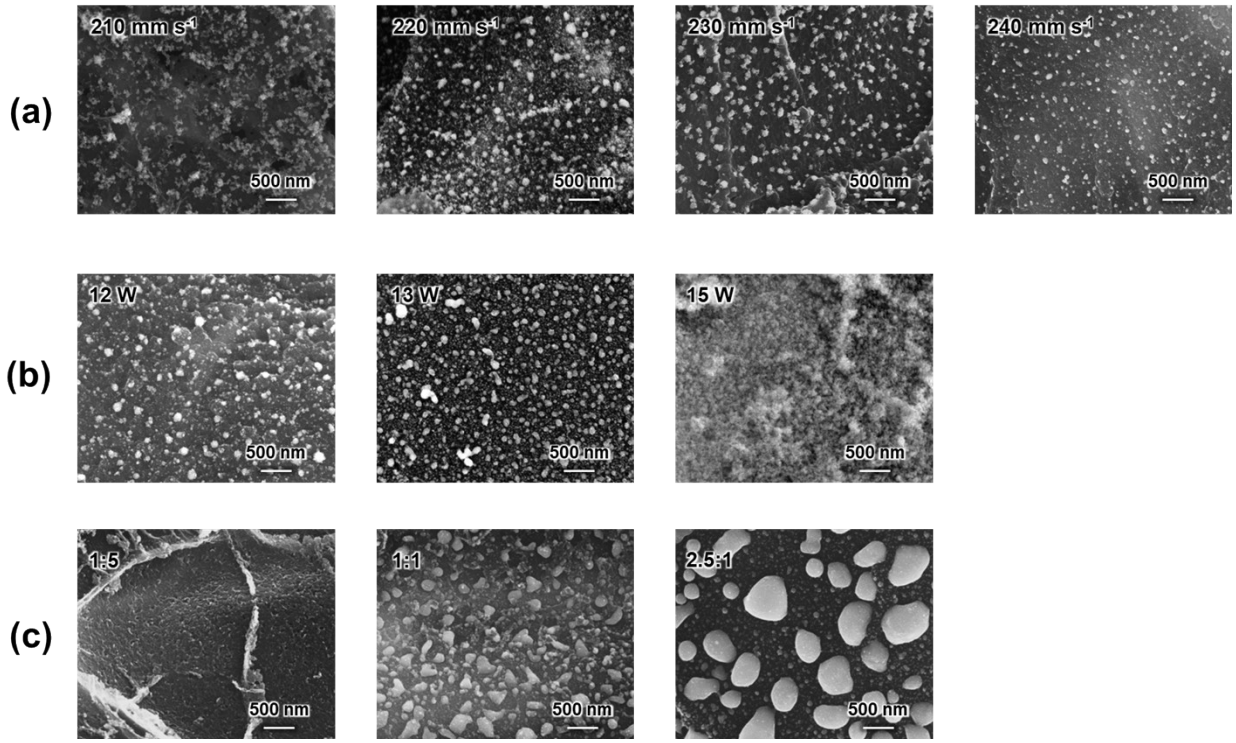

Fig. S2. SEM image in mixed mode between SE (Secondary Electrons) and BSE (Backscattered Electrons) mode of the PdNPs formed at (a) various laser scan speed (210, 220, 230, and 240 mm s^{-1}) while keeping the laser power fixed at 14 W and precursor ratio at 1:2.5. (b) at laser powers (12, 13, and 15 W) while keeping the scan speed fixed at 220 mm s^{-1} and precursor ratio at 1:2.5. (c) at the precursor ratio (1:5, 1:1, and 2.5:1 v/v) while keeping the scan speed and laser power fixed at 220 mm s^{-1} and 14 W, respectively.

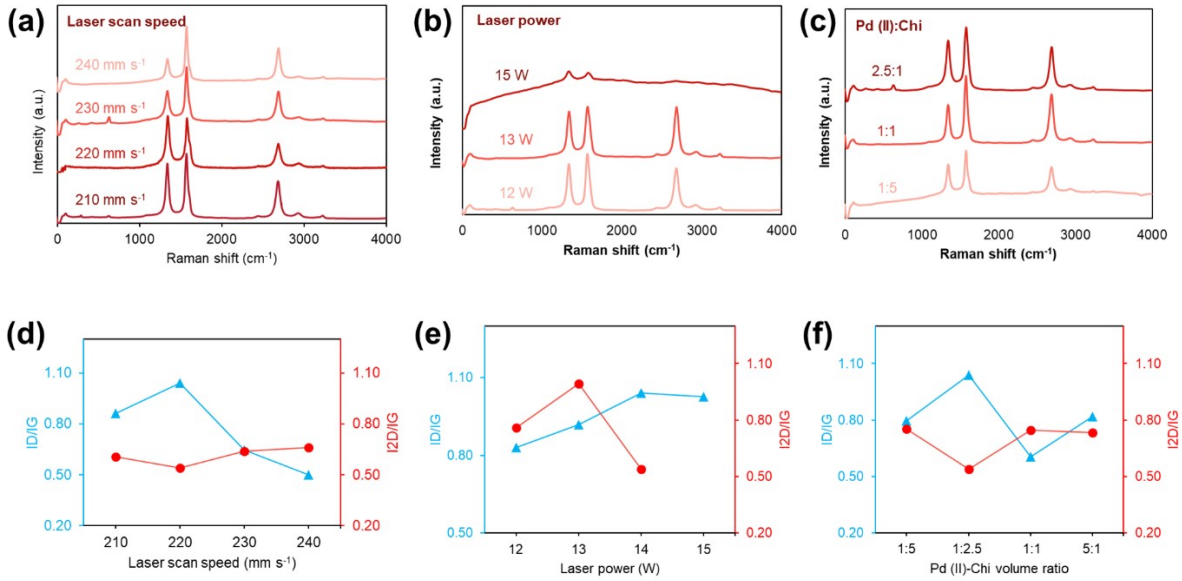

Fig. S3. Raman spectra and the intensity ratio (I_D/I_G and I_{2D}/I_G) of nanoPd@LIG with different (a and d) laser scan speed 210−240 mm s^{-1} , (b and e) laser power 12 – 15 W, and (c and f) Pd(II):Chi ratio of 1:5, 1:2.5, 1:1 and 2.5:1.

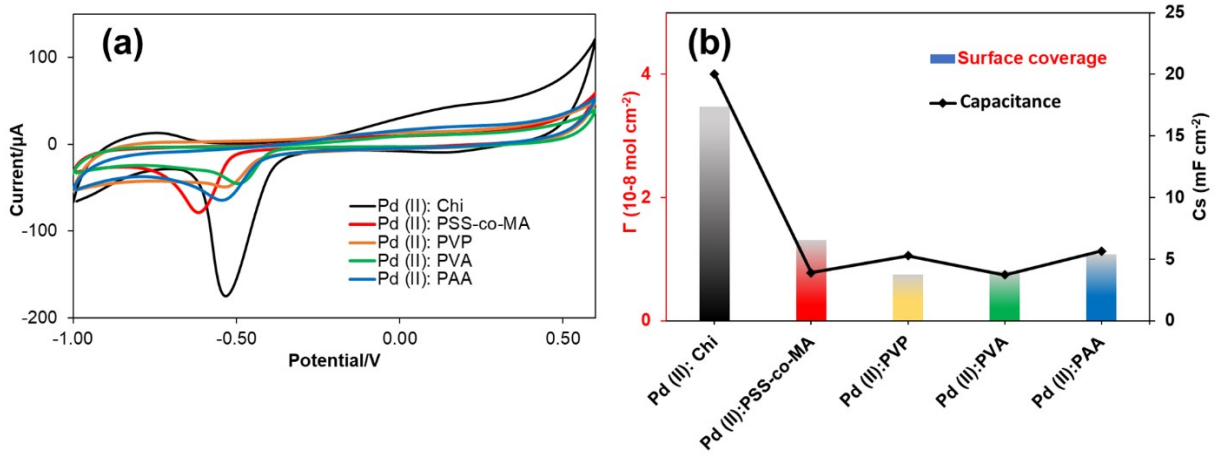

Fig. S4. (a) Cyclic voltammograms and (b) surface coverage of the catalytic activity and specific capacitance value of nanoPd@LIG nanocomposites fabricated using different polymers in the polymer–Pd(II)- precursor.

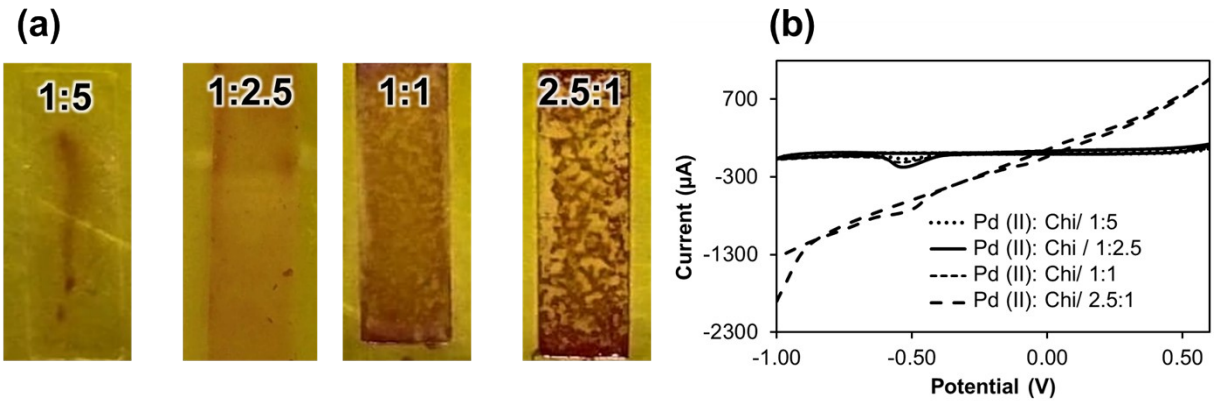

Fig. S5. (a) Photograph of top view laser irradiated Chi–Pd (II) precursors at different ratios. (b) Cyclic voltammograms of nanoPd@LIG synthesized at different Chi–Pd (II)ratios.

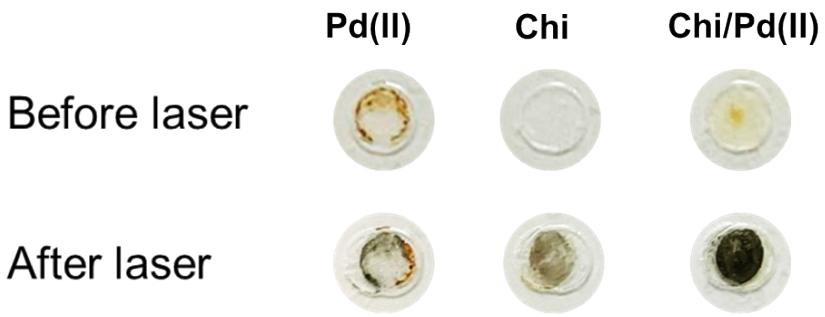

Fig. S6. Photographs of Pd (II), Chi, and Chi/Pd (II) film on glass slides before and after laser irradiation.

Equation S1:

$$\Psi = \frac{-0.6288 + 0.0021\Delta E_p}{1 - 0.017\Delta E_p} \quad \text{(S1)}$$

Equation S2:

$$\Psi = \frac{k^0_{eff}}{\left(\frac{n\pi FD\nu}{RT}\right)^{\frac{1}{2}}} \quad \text{(S2)}$$

k^0_{eff} is heterogeneous electron transfer standard rate constant

Ψ is kinetic parameter obtained from scan rate (ν)-dependent cyclic voltammograms

n is the number of electrons transferred

F is the Faraday's constant

υ is the scan rate (V s^{-1})

R is the universal gas constant

T is temperature (K)

D is the diffusion coefficient of the redox probe

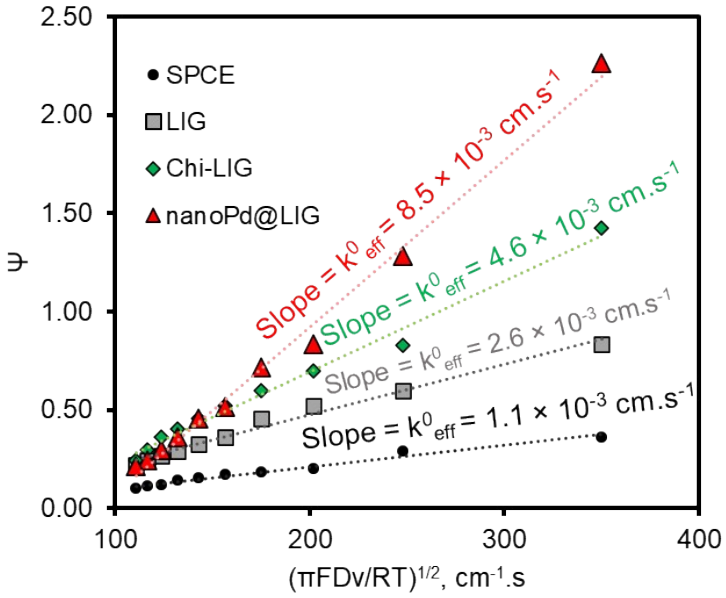

Fig. S7. HET kinetic analysis within the scan rate range of 10–100 mV s^{-1}, showing the kinetic parameter Ψ obtained via Eq. (S1), along with the linear regression for the estimation of the effective HET standard rate constant, k^0_{eff}, via Eq. (S2).

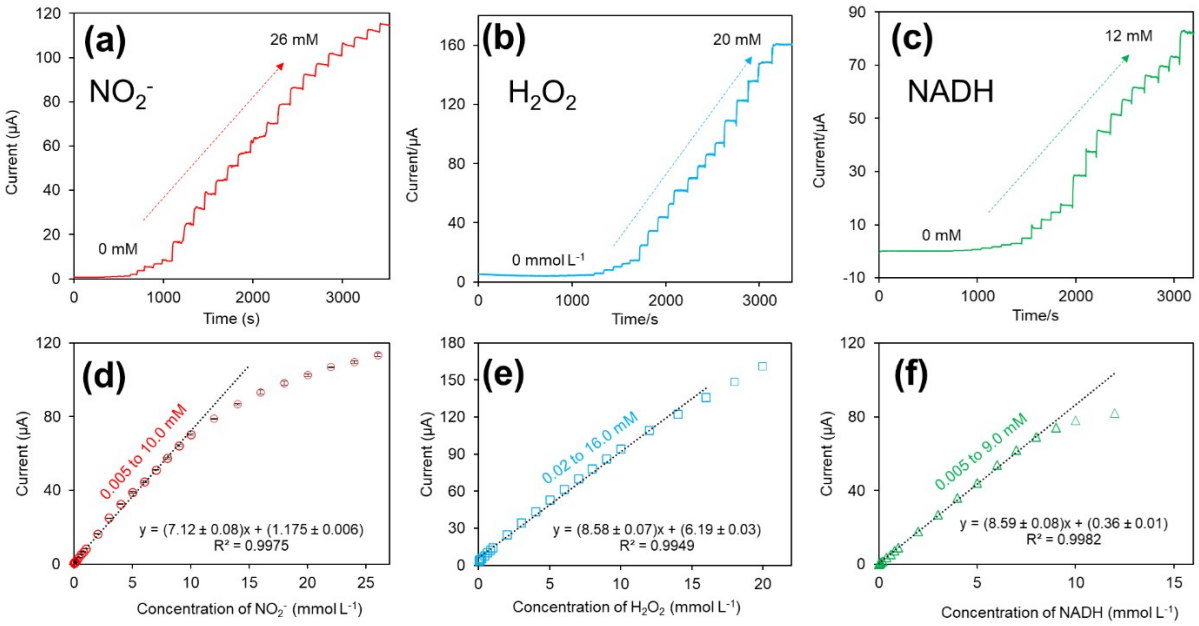

Fig. S8. The i-t curves and the corresponding calibration plots of nanoPd@LIG in a 0.10 mol L^{-1} PB (pH 7.4) after successive additions of different concentrations of (a and d) NO_2^- from 0 to 26 mmol L^{-1} at 0.68 V (vs. pseudo-Ag/AgCl); (b and e) H_2O_2 from 0 to 20 mmol L^{-1} at 0.58 V (vs. pseudo-Ag/AgCl); and (c and f) NADH from 0 to 12 mmol L^{-1} at 0.28 V (vs. pseudo-Ag/AgCl).

Fig. S9. Digital images of nanoPd@LIG in multi-working electrode and three-electrode systems.

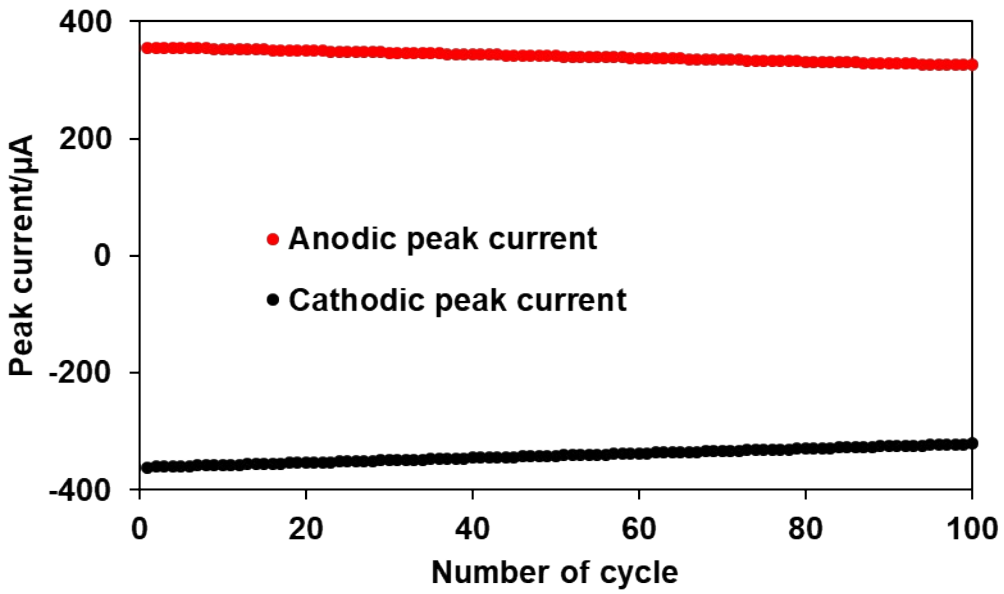

Fig. S10. Stability of nanoPd@LIG electrode in 5 mmol L^{-1} $[Fe(CN)_6]^{3-/4-}$ containing 1.0 mol L^{-1} KCl via CV tests with consecutive 100 cycles.

Table S1. Summary of laser parameter optimization.

Laser scan speed (mm s^{-1})	Γ (10^{-8} mol cm^{-2})	PdNPs size (nm)	Cs (mF cm^{-2})	Pore size (μm)	Percentage of the element (%)		
					C	Pd	Pd/C
210	2.2 ± 0.1	102 ± 34	13.1	5 ± 2	87.4	8.3	0.095
220	3.4 ± 0.1	94 ± 30	20.0	3.5 ± 0.9	84.3	11.8	0.140
230	2.7 ± 0.1	92 ± 29	13.2	3.4 ± 1	88.9	8.5	0.096
240	1.8 ± 0.6	77 ± 24	9.6	5 ± 2	93.3	3.9	0.042
Laser power (W)	Γ (10^{-8} mol cm^{-2})	PdNPs size (nm)	Cs (mF cm^{-2})	Pore size (μm)	Percentage of the element (%)		
					C	Pd	Pd/C
12	1.56 ± 0.08	98± 50	7.479	3 ± 1	90.0	4.2	0.047
13	2.0 ± 0.1	105 ± 50	14.016	3 ± 1	91.5	5.5	0.060
14	3.3 ± 0.2	94 ± 30	20.027	3.5 ± 0.9	84.3	11.8	0.140
15	1.3 ± 0.4	Cannot measure	17.587	10 ± 6	72.4	3.5	0.048
Ratio of Pd (II): Chi (V/V)	Γ (10^{-8} mol cm^{-2})	PdNPs size (nm)	Cs (mF cm^{-2})		Percentage of the element (%)		
					C	Pd	Pd/C
1:5	1.00 ± 0.05	Cannot measure	10.5		92.6	2.9	0.031
1:2.5	3.3 ± 0.2	94 ± 30	20.0		84.3	11.8	0.140
1:1	1.8 ± 0.3	159 ± 76	18.0		77.9	15	0.193
2.5:1	1.1 ± 0.3	257 ± 253	-		53.5	45	0.841

Table S2. Summary of thickness of the LIG layers using thickness analyzer (Mitutoyo, model 543-790B, Japan) on laser parameter.

Scan speed (mm s^{-1})	Thickness (μm)
210	14 ± 4
220	17 ± 1
230	20 ± 5
240	24 ± 2
Laser power (W)	
12	21 ± 2
13	17 ± 2
14	16 ± 1
15	Crack

Table S3. Summary of characteristic bands present in Raman spectra.

Electrode		D	G	2D	D/G	2D/G
LIG	Position	1346.5	1578.9	2695.2	0.80	0.61
	Intensity	1701	2136.5	1293		
	FWHM	40.4	21.0	58.3		
Chi@LIG	Position	1346.4	1578.8	2693.1	0.40	0.46
	Intensity	1762	4368	2026		
	FWHM	48.0	32.39	50.1		
nanoPd@LIG	Position	1344.1	1578.9	2690.3	1.04	0.54
	Intensity	2683.3	2580.3	1391.6		
	FWHM	49.1	65.0	65.9		

Table S4. Analytical performance of the nanoPd@LIG electrode for NO_2^-, H_2O_2, and NADH detection.

Analyte	Linear range (mmol L^{-1})	Sensitivity (μA L $mmol^{-1}$ cm^{-2})	LOD (μmol L^{-1})
NO_2^-	0.005 – 10.0	101	2.5
H_2O_2	0.02 – 16.0	122	17.2
NADH	0.005 – 9.0	64	3.4